J. Electrochem. Sci. Eng. **13(5)** (2023) 739-751; http://dx.doi.org/10.5599/jese.1699

Open Access : : ISSN 1847-9286
https://pub.iapchem.org/ojs/index.php/JESE

Short communication

Feasibility study of amperometric and electrochemical quartz crystal microbalance measurements for *in situ* state of charge monitoring in vanadium flow batteries

Claudia Weidlich[1,✉], Felix Lulay[1,2], Matthias Wieland[1]

[1]*DECHEMA-Forschungsinstitut, Theodor-Heuss-Allee 25, 60486 Frankfurt, Germany*

[2]*Centre for Electrochemical and Surface Technology, Viktor-Kaplan-Strasse 2, 2700 Wr. Neustadt, Austria*

Corresponding author: ✉*claudia.weidlich@dechema.de; Tel.: +49 69 7564 633; Fax: +49 69 7564 388*

Received: February 13, 2023; Accepted: May 14, 2023; Published: May 31, 2023

Abstract

For an efficient flow battery operation, knowledge of the state of charge of the battery is essential. Monitoring the state of charge of both half cells is advantageous concerning a timely detection of crossover processes. We present the first results for amperometric and electrochemical quartz crystal microbalance measurements in a vanadium flow battery test setup. By validating with half cell potential measurements as well as ex situ titration we investigated the applicability of both electrochemical methods for an in situ half cell state of charge monitoring.

Keywords

Crossover; half cell; electrolyte properties

Introduction

To overcome the challenges to mitigate climate change, the storage of renewable energies is essential. Flow batteries (FB) are most suitable to store wind or solar energy due to the characteristic independent scalability of energy and capacity [1,2]. Of all FB chemistries, all-vanadium flow batteries (VFB) are most common and commercially prevailed. They contain vanadium electrolyte in the negative half cell (NHC) as well as the positive half cell (PHC) [3]. The charging (from left to right) and discharging (from right to left) processes of the NHC and PHC are characterised by reactions (1) and (2):

$$V^{3+} + e^- \rightleftarrows V^{2+} \text{ (NHC)} \quad (1)$$

$$VO^{2+} + H_2O \rightleftarrows VO_2^+ + e^- + 2H^+ \text{ (PHC)} \quad (2)$$

During charging, V(III) ions are reduced to V(II) in the NHC while the oxidation of V(IV) ions to V(V) occurs in the PHC. During discharging V(III) ions and V(IV) ions are formed in the NHC and PHC, respectively. The crossing of vanadium species through the ion exchange membrane, which separates

the PHC from the NHC, does not lead to a contamination of the half cell electrolytes since both half cells contain vanadium. However, the battery half cells are suffering from self discharge. Furthermore, the half cell electrolytes may undergo other reversible and also irreversible changes as *e.g.* concentration changes due to osmotic processes, overoxidation and electrolysis of the electrolyte [4-8]. Therefore, knowledge of the state of charge (SOC) of the battery is necessary for an efficient operation of the VFB. In commercial VFB the so called reference cell monitoring is widely used [4-9] but this monitoring method is limited to the determination of the SOC of the full cell electrolyte and does not give information about electrolyte crossover and self discharge of the battery half cells.

Monitoring SOC of each half cell separately is much more suitable than reference cell monitoring for a timely detection of crossover and other processes which alter the half cell electrolytes. Since, next to oxidation state of the electroactive vanadium species, several electrolyte properties such as concentration, conductivity, pH, density, viscosity and absorbance may change during charge and discharge, numerous measurement methods are suitable [1] for an *in situ* detection of these changes. Monitoring the redox potential of the half cells using reference electrodes [4,5,9-11] as well as using UV/Vis spectroscopy [12-15] to monitor the oxidation state and concentration of the vanadium ions the half cell electrolytes have been widely investigated. In addition to that, density measurements [10], viscosity measurements [16] and distribution of relaxation times (DRT) analysis applied on electrochemical impedance spectroscopy (EIS) data [17] have been implemented to investigate the VFB electrolyte *in situ*.

Amperometric measurements might be suitable for a novel *in situ* half cell monitoring in VFB. This method has already been studied for *ex situ* and *in situ* monitoring using microelectrodes in organic FB [3,18-20]. Various potentials have been applied and the ratio of resulting oxidation and reduction currents has been plotted vs. the ratio of the concentration of the oxidized and reduced species in the electrolyte. An outstanding advantage of this approach is the independence on temperature, electrolyte composition and concentration [18]. For VFB, the suitability of amperometric measurements using working electrodes coated with porous diffusion layers for an *ex situ* determination of the SOC, has been shown [2] and also an electro catalytic metal electrode for estimating the SOC of the positive electrolyte has been patented [21].

Also, the electrochemical quartz crystal microbalance (EQCM) might be suitable for SOC monitoring. An EQCM consists of a quartz crystal in contact with electrodes on both sides of the quartz which stimulate oscillation. The electrode facing the electrolyte is also contacted as working electrode to a potentiostat. Simultaneously with the changes in oscillation frequency of the quartz crystal, electrochemical reactions can be analysed at the electrode [22]. EQCM has been already used for density and viscosity measurements [23,24] and battery monitoring in general [25] as well as for measuring density and viscosity in lead acid batteries in particular [26]. EQCM therefore provides the possibility to investigate two different electrolyte parameters as redox potential and viscosity at the same time within the same setup [25].

We are investigating these two different electrochemical methods according to their feasibility for SOC monitoring in VFB.

Experimental

The battery test setup for this study contains the battery cell and a tank for each battery half cell. The electrolyte is pumped with 1.5 – 2.1 l/h electrolyte flow using a membrane pump (ProMinent, delta opto drive). The battery cell with an electrode area of 10 cm^2 has been manufactured by the machine shop at the DECHEMA-Forschungsinstitut and is equipped with a F10100 membrane

(Fumatech BWT GmbH), GFD 4.6 EA electrode felts (SGL Carbon) and SP4369 bipolar plates (Schunk Kohlenstofftechnik GmbH). Commercial vanadium electrolyte (GfE Metalle und Materialien GmbH) with a vanadium concentration of 1.6 M and acid concentration of 2 M is used. For charge and discharge experiments volumes between 60 and 150 ml electrolyte are filled in each tank. The battery cycling is performed under argon with charge/discharge currents of 50 or 100 mA cm^{-2} and voltage criteria of +1.65V (charged) and +0.8 V (discharged) using a Gamry Reference 3000AE Potentiostat/Galvanostat. The components and parameters described have been utilized both for the amperometric and EQCM measurements. Additionally, each half cell electrolyte circuit is equipped with a flow cell to measure open circuit potential (OCP) of the half cell electrolyte. Both flow cells are connected by an electrolyte bypass to the battery test setup and the electrolyte is pumped through the bypass using a ISM796 peristaltic pump (Ismatec). A glassy carbon (GC) rod with 2 mm diameter (Sigradur D, Hochtemperatur-Werkstoffe GmbH) and a Hg/Hg_2SO_4 reference electrode (Xylem Analytics Germany Sales GmbH & Co. KG) in a Luggin capillary (filled with 2 M H_2SO_4) are mounted in each flow cell to measure OCP. Figure 1 provides a scheme for the test set up with cells for OCP (insertion in the middle), amperometric (insertion right) and EQCM (insertion left) measurements. The electrochemical cells used for amperometric and EQCM measurements are described below.

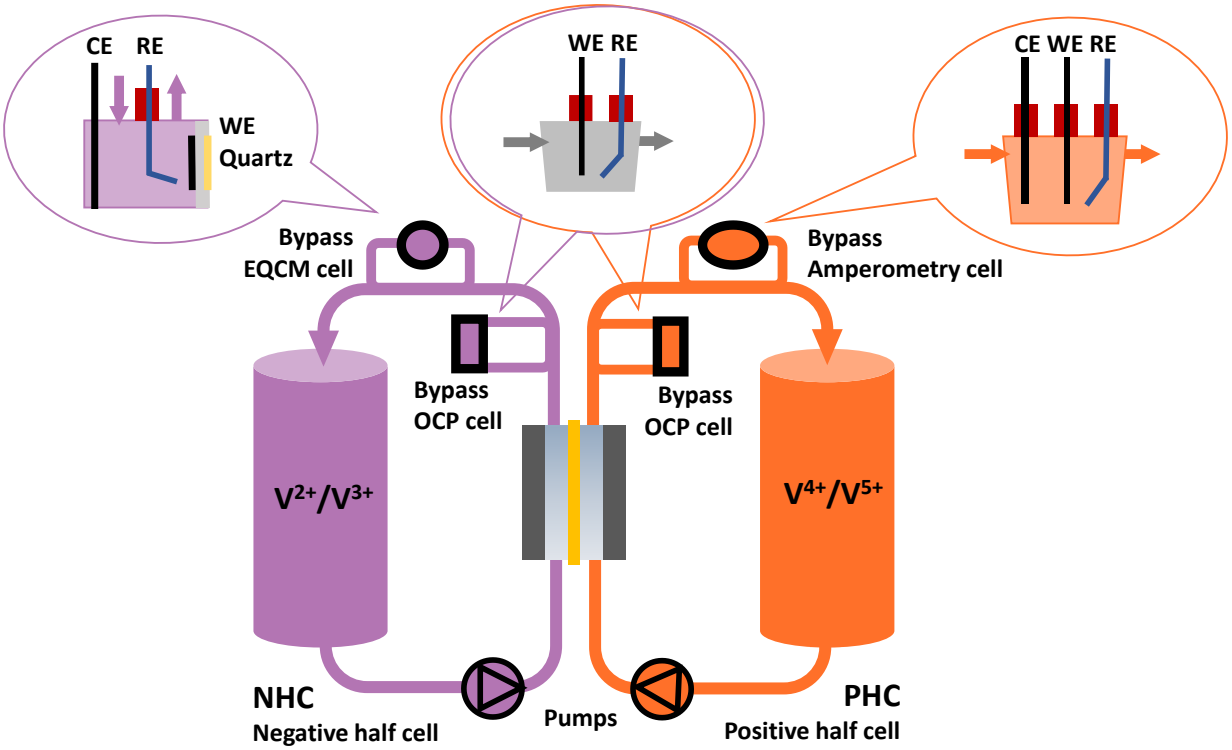

Figure 1. *Scheme for VFB test setup with electrochemical cells for in situ amperometric measurements in the positive half cell (PHC) and in situ electrochemical quartz crystal microbalance (EQCM) measurements in the negative half cell (NHC). Open circuit potential (OCP) measurements. Cells equipped with electrodes: working (WE), reference (RE) and counter (CE)*

Ex situ calibration of the mentioned monitoring methods has been done using potentiodynamic titration (Titrando 888, Deutsche METROHM GmbH & Co. KG) with 0.1 M $Ce(SO_4)_2$ (Carl Roth GmbH & Co. KG). As sensor, a platinum indicator electrode has been utilized for all measurements (Combined iPt ring electrode, Deutsche METROHM GmbH & Co. KG). The equivalence points have been calculated with Tiamo *v*2.5 (Deutsche METROHM GmbH & Co. KG).

The concentration of V^{4+} has been determined by titration using $Ce(SO_4)_2$. Afterwards $FeSO_4$-heptahydrate has been added until the potential dropped below 550 mV relative to the sensor

electrode to ensure that V^{5+} is reduced quantitatively. Therewith, the total concentration of vanadium in the positive electroyte has been titrated using $Ce(SO_4)_2$. V^{5+} concentration has been calculated as the difference of the total vanadium concentration and V^{4+} concentration. The SOC has been determined as the proportion of V^{5+} on the total vanadium concentration.

Amperometric measurements are tested (using a Gamry Reference 3000AE Potentiostat/Galvanostat) concerning their feasibility for SOC monitoring at VFB and several setup configurations have been applied:

A. *Ex situ* three-electrode setup using a carbon microelectrode as working electrode (carbon fibre with 33µm diameter, MCE Micro Carbon fiber electrode, ALS Co., Ltd.), Hg/Hg_2SO_4 reference electrode (Xylem Analytics Germany Sales GmbH & Co. KG) in a Luggin capillary (filled with 2 M H_2SO_4) and a glassy carbon rod counter electrode with 2 mm diameter (Sigradur D, Hochtemperatur-Werkstoffe GmbH), all electrodes installed in a small glass cell (20 ml cell volume). The battery has been operated with 100 ml electrolyte in the NHC tank and 60 ml in the PHC tank to ensure full charging and discharging of the PHC electrolyte. During battery charge and discharge at several SOC, 1 ml electrolyte has been withdrawn from the tank of the PHC, added to the amperometric cell subsequently mixed with 2 ml ultrapure H_2O. Another 0.5 ml electrolyte has been withdrawn from the tank to determine the SOC by titration (see paragraph above). For the ~~c~~amperometric measurement, a reduction potential of (-1.2 V *vs.* Hg/Hg_2SO_4) has been applied to the microelectrode for 30 s and then an oxidation potential of (+1.0 V vs. Hg/Hg_2SO_4) has been applied for 30 s. Reduction and oxidation have been applied in an alternating manner several times (see Fig. 4). All amperometric measurements have been conducted under argon protection.

B. *In situ* three-electrode setup using a carbon microelectrode as working electrode (carbon fiber with 33 µm diameter, ALS Co.,Ltd.), Hg/Hg_2SO_4 reference electrode (Xylem Analytics Germany Sales GmbH & Co. KG) in a Luggin capillary (filled with 2 M H_2SO_4) and a glassy carbon rod as counter electrode with 2 mm diameter (Sigradur D, Hochtemperatur-Werkstoffe GmbH). The amperometric cell has been connected to the electrolyte bypass with two hoses, one for filling and one for emptying the amperometric cell. In order to carry out the amperometric measurement, the cell has been filled up to a level which was constant for all measurements (7 ml) and convection has been avoided. A reduction potential of (-1.2 V *vs.* Hg/Hg_2SO_4) has been applied for 30 s and an oxidation potential of (+1.0 V vs. Hg/Hg_2SO_4) has been applied for 30 s. After the amperometric measurement, 0.5 ml electrolyte has been withdrawn from the cell for SOC determination via titration. Afterwards, the electrolyte in the amperometric cell has been pumped back through the bypass to the electrolyte circuit. This “stop and flow” methode for electrolyte sampling in the amperometric cell has also been used for setup C and D.

C. *In situ* three-electrode setup using a glassy carbon rod as working electrode with 2 mm diameter (Sigradur D, Hochtemperatur-Werkstoffe GmbH), Hg/Hg_2SO_4 reference electrode (Xylem Analytics Germany Sales GmbH & Co. KG) in a Luggin capillary (filled with 2 M H_2SO_4) and a glassy carbon rod counter electrode with 2 mm diameter (Sigradur D, Hochtemperatur-Werkstoffe GmbH). The setup and the measurement are described in B. A reduction potential of (-0,7 V vs. Hg/Hg_2SO_4) has been applied for 30 s and an oxidation potential of (+0.9 V vs. Hg/Hg_2SO_4) has been applied for 30 s.

D. *In situ* two-electrode setup using a glassy carbon rod as working electrode and a second glassy carbon rod counter electrode with 2 mm diameter (Sigradur D, Hochtemperatur-Werkstoffe

GmbH). The setup and the measurement are described in B. A reduction potential of (-1.0 V) has been applied for 30 s and an oxidation potential of (+0.7 V) has been applied for 30 s.

The electrochemical quartz crystal microbalance (EQCM) consists of a commercially available cell case (Deutsche METROHM GmbH & Co. KG) in which the quartz crystal is inserted. A carbon plate has been installed as a counter electrode (CE). The cell head has been manufactured to work as a flow cell. Electrolyte inlet and outlet and the Luggin capillary with Hg/Hg_2SO_4 reference electrode (Xylem Analytics Germany Sales GmbH & Co. KG) have been connected to the cell head. After assembling the cell, it has been connected to the electrolyte bypass circuit and filled from the bottom and emptied from the top in order to avoid accumulation of bubbles on the electrodes.
The EQCM cell has been connected to the bypass electrolyte of the NHC and the oscillation frequency of the crystal and the potential between the carbon coated crystal and Hg/Hg_2SO_4 RE (OCP) have been monitored during battery cycling. For controlling the EQCM experiment, a PGSTAT302N Potentiostat (Deutsche METROHM GmbH & Co. KG) and gold coated quartz crystals with a thin layer of carbon evaporated onto one side (6 MHz resonance frequency, RenLux Crystals Ltd.) serving as working electrode in the EQCM cell have been utilised. Carbon has been applied as coating material to mimic the carbon electrodes used in VFB.

The battery cell has been cycled between 0.8 and 1.65 V with a current density of 50 mA cm^{-2} during the EQCM experiments.

Results and discussion

The VFB in the test setup has been charged and discharged using the parameters described above. Figure 2 shows exemplary operation of the battery cell respectively the resulting potentials during charging and discharging with 50 mA cm^{-2}. The VFB is running stable, and the charge/discharge cycles are reproducible. Since the battery has been operated with an excess of NHC electrolyte to ensure full charging and discharging of the PHC electrolyte, a slightly increasing duration of the cycles can be observed which is due to crossover of NHC electrolyte through the cation exchange membrane and therefore capacity increase in the PHC.

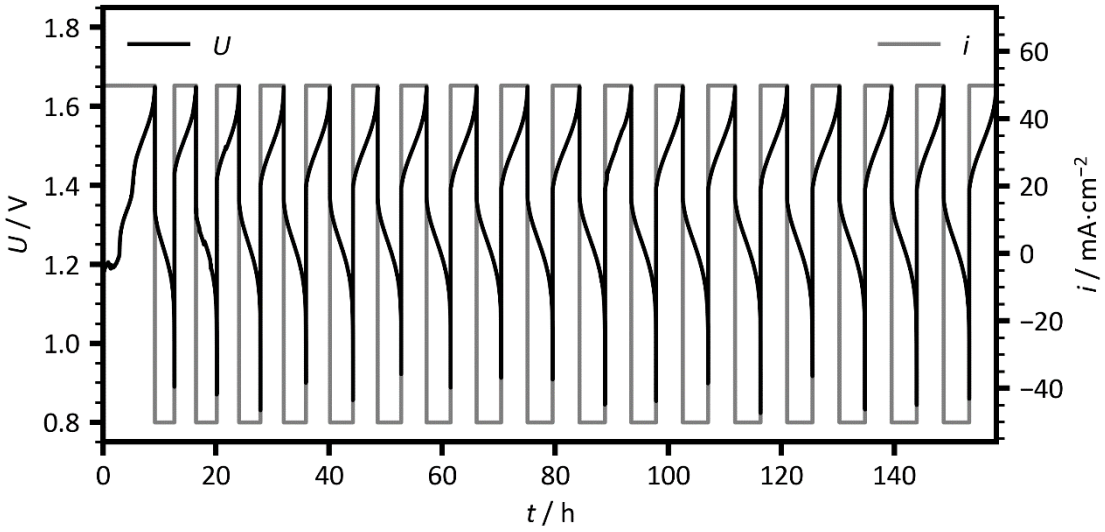

Figure 2. *Cycling of the VFB test setup (10 cm^2 battery cell) with 50 mA cm^{-2}*

During cycling of the battery cell, the open circuit potential (OCP) has been monitored for both half cells using flow cells equipped each with a GC rod and a Hg/Hg_2SO_4 reference electrode. Figure 3 shows the SOC calculated from OCP measured in the positive half cell (PHC) (grey curve) in

comparison to the SOC calculated from the titration of samples taken from PHC electrolyte during the amperometric measurements. The SOC calculated from *in situ* OCP measurements in the PHC is in good accordance with the SOC determined by titration (black crosses).

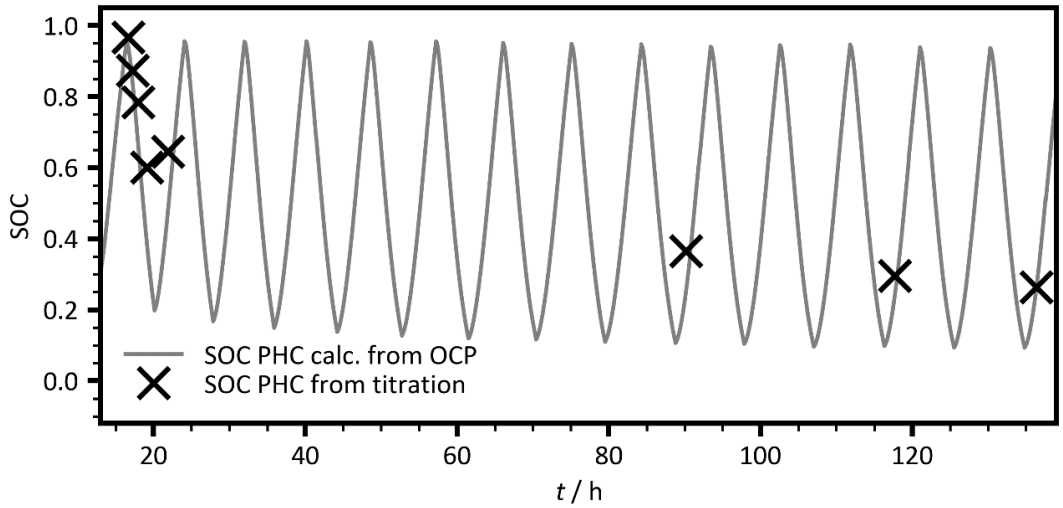

Figure 3. *State of charge (SOC) calculated from open circuit potential (OCP) measurements in the positive half cell (PHC) and SOC calculated from titration (black crosses)*

The titration samples have been taken from the PHC and analysed directly after several amperometric meaurements. The results for these measurements are described below and are shown in Figures 4 and 5.

Amperometric measurements

At first, the three-electrode setup using a carbon microelectrode (A) has been tested *ex situ* to ensure a convection-free measurement at the microelectrode.

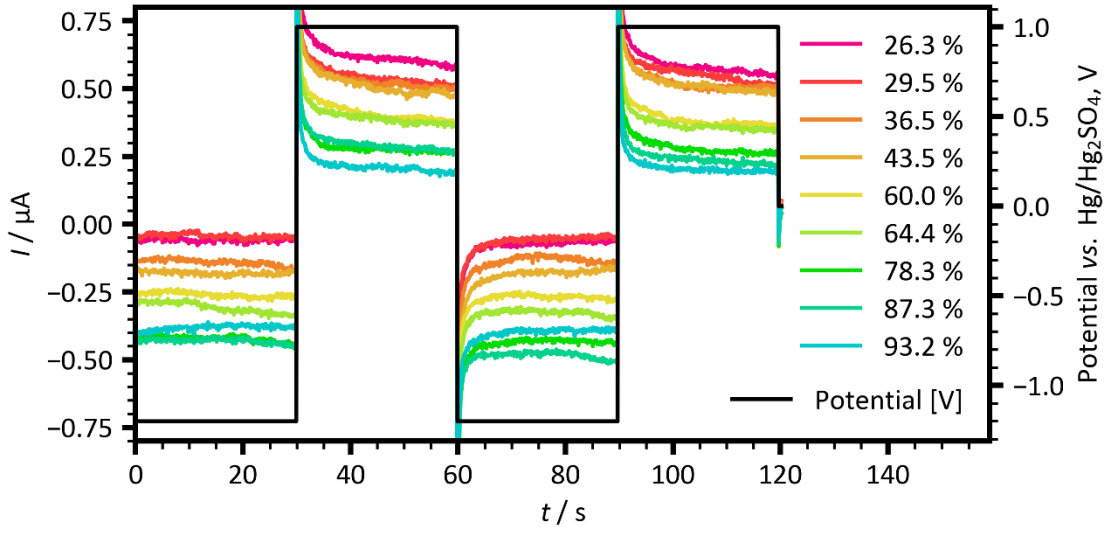

Figure 4. *Ex situ amperometric measurements at the positive half cell with three-electrode setup using a microelectrode*

Figure 4 shows that for the amperometric experiments the reduction current resulting from polarisation with -1.2 V increases with increasing SOC whereas the oxidation current resulting from polarisation with +1.0 V decreases with increasing SOC. Since in the PHC the share of vanadium ions in the charged state (V^{5+}) increases with SOC, the reduction current increases because the amount of reducible vanadium ions increase. *Vice versa*, the oxidation current decreases with increasing SOC

since the amount of oxidisable V^{4+} ions decrease. The currents measured for the reduction and oxidation steps are reproducible. The average of the last 10 seconds of the measured currents is referred to as oxidation/reduction current and the ratio $\ln(I_{ox}/I_{red})$ is calculated according to [3,18].

The ln for the ratio of the measured oxidation and reduction current is supposed to linearly depend on the ln for the concentration of the oxidised and reduced vanadium ions in the electrolyte [18]. According to theory, an equal share of oxidised and reduced species ($\ln(c_{ox}/c_{red}) = 0$) should result in equal oxidation and reduction currents ($\ln(I_{ox}/I_{red}) = 0$). Plotting the raw data, it has been observed that all data points are shifted towards higher $\ln(c_{ox}/c_{red})$ values, which has also been observed for all amperometric measurements. Because of that, all measured currents have been corrected by the *y*-intercept of the linear regressions calculated for each set of oxidative and reductive currents, respectively, according to [18]. Nevertheless, the slope of the regression line is expected to be -1 for all experiments.

Within the following the $\ln(I_{ox}/I_{red})$ vs. $\ln(c_{ox}/c_{red})$ plots for the corrected currents are shown and discussed. The plot of $\ln(I_{ox}/I_{red})$ as determined by amperometric measurements *vs.* $\ln(c_{ox}/c_{red})$ as determined by titration (as explained in the Experimental section) is shown in Figure 5. For easier understanding, the SOC values calculated from titration results are added.

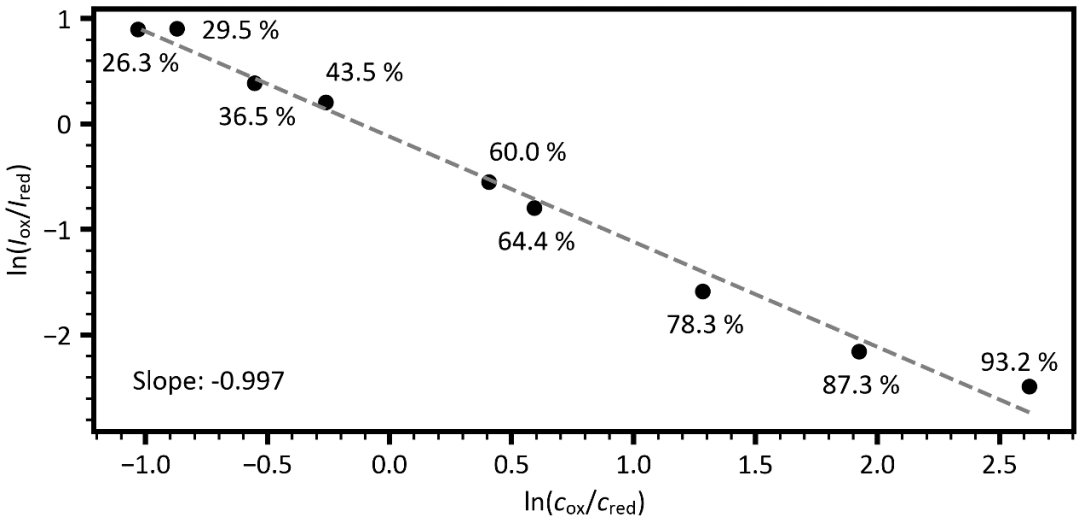

Figure 5. *ln(I_{ox}/I_{red}) vs. ln(c_{ox}/c_{red}) plot for ex situ amperometric measurements at the positive half cell with three-electrode setup using a microelectrode*

Figure 5 reveals that $\ln(I_{ox}/I_{red})$ linearly depends on $\ln(c_{ox}/c_{red})$ with a slope of nearly -1.

To investigate the applicability of this setup for *in situ* monitoring, the amperometric cell was connected to the PHC electrolyte circuit and operated as described in B.

In Figure 6, the results for the *in situ* three-electrode setup using a carbon microelectrode (B) are shown and the SOC calculated from titration is added. The results are in good accordance to the results for the *ex situ* three-electrode setup using the microelectrode. The regression line again shows a slope of nearly -1.

Since a microelectrode might be susceptible for interferences when applied in a technical VFB system, an *in situ* three-electrode setup using a GC rod (C) working electrode has been tested in order to simplify and to optimise the amperometric setup regarding maintenance and cost efficiency.

Figure 7 shows that, using a GC rod working electrode, $\ln(I_{ox}/I_{red})$ also results in a linear dependency on $\ln(c_{ox}/c_{red})$ with a slope of nearly -1. Comparing Figures 4, 5 and 6, differences in the scaling of the axis for $\ln(I_{ox}/I_{red})$ and $\ln(c_{ox}/c_{red})$ are due to different SOC ranges in which the experiments have been done and samples have been taken.

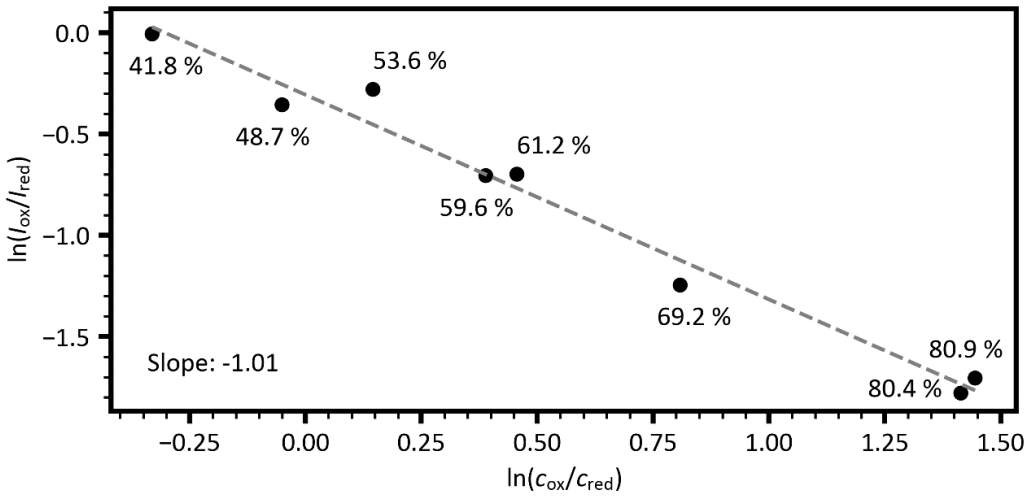

Figure 6. *ln(I_{ox}/I_{red}) vs. ln(c_{ox}/c_{red}) plot for in situ amperometric measurements at the positive half cell with three-electrode setup using a microelectrode*

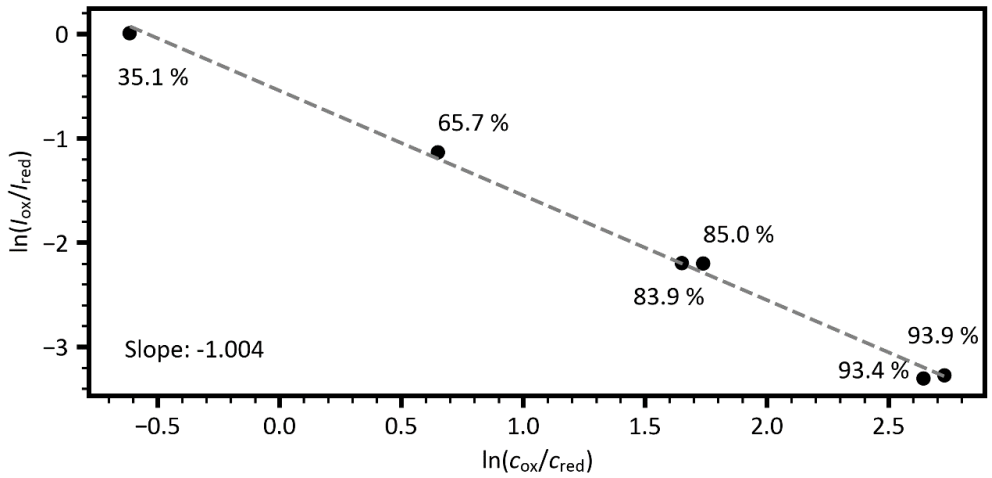

Figure 7. *ln(I_{ox}/I_{red}) vs. ln(c_{ox}/c_{red}) plot for in situ amperometric measurements at the positive half cell with three-electrode setup using a glassy carbon rod working electrode*

For comparison, in Figure 8 the results for (I_{ox}/I_{red}) are plotted *vs.*(c_{ox}/c_{red}) to reveal an exponential dependency and the necessity to plot the natural logarithms to yield a linear calibration.

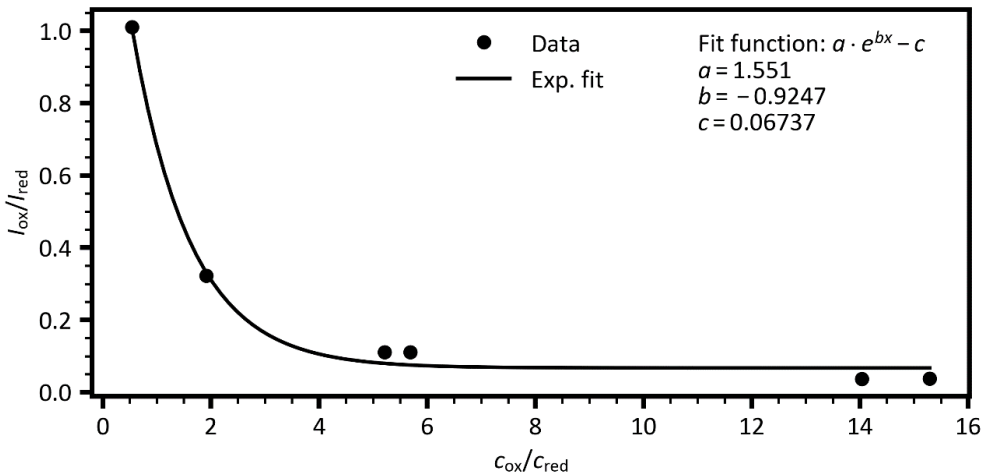

Figure 8. I_{ox}/I_{red} vs. c_{ox}/c_{red} *plot for in situ situ amperometric measurements at the positive half cell with three-electrode setup using a glassy carbon rod*

For further simplification and cost reduction, the reference electrode has been omitted and the results for amperometric measurements with an *in situ* two-electrode setup using a GC rod (D) working electrode are shown in Figure 9. The results reveal that also for this simplified setup the results are in good accordance to the results gained for the three-electrode setup using a microelectrode. The results for $\ln(I_{ox}/I_{red})$ still show a linear dependency on $\ln(c_{ox}/c_{red})$ but with a slope which deviates slightly stronger from -1. This might be caused by a potential shift at the glassy carbon rods during the experiment.

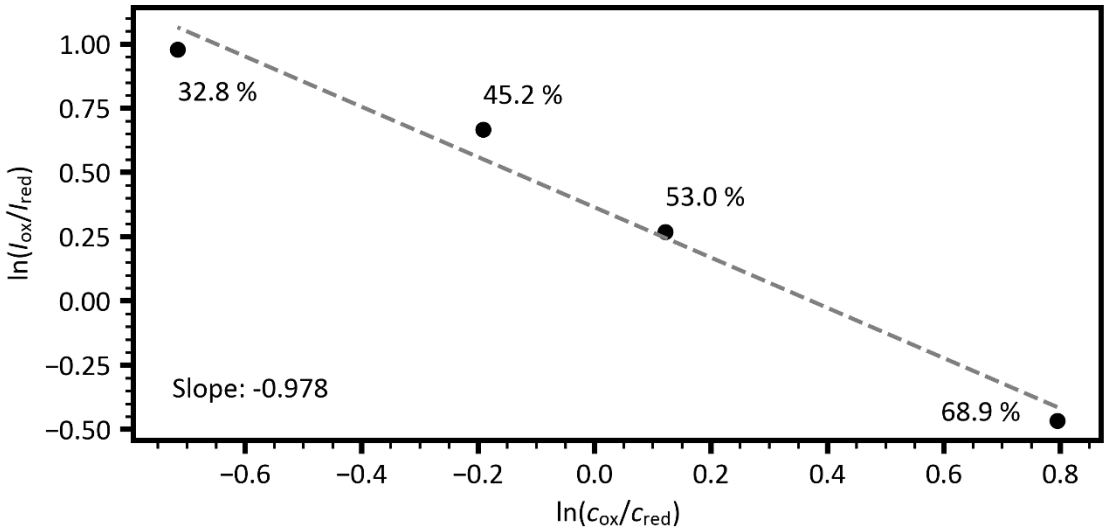

Figure 9. *ln(I_{ox}/I_{red})* vs. *ln(c_{ox}/c_{red}) plot for in situ amperometric measurements at the positive half cell with 2-electrode setup using glassy carbon rods*

In addition, we also have been testing the electrochemical quartz crystal microbalance (EQCM) concerning its applicability for SOC monitoring. The quartz crystal coated with a carbon layer as working electrode on one side can be utilized to measure OCP in the electrolyte circuit and furthermore measuring the oscillation frequency may allow the investigation of electrolyte properties as density and viscosity at the same time respectively within the same setup. To check the applicability, an EQCM cell has been mounted in a bypass of the NHC electrolyte circuit of the VFB test setup and the battery cell has been charged and discharged. Figure 10 (a) shows that the results for OCP measured at the carbon coated quartz crystal and OCP measured at the GC rod in the flow cell are comparable and in good accordance. Figure 10 (b) shows the frequency of the crystal which has been measured simultaneously and also in a currentless state. The results reveal that changes of the frequency of the oscillating quartz crystal depend on the SOC of the electrolyte. High frequencies which are expected to be measured for low electrolyte densities are observed for high OCP respectively high SOC of the NHC. This is in good accordance to results published for VFB electrolyte densities in dependence on SOC [10]. For the charged state of the NHC, the density of the electrolyte is low which results in high frequencies whereas the higher electrolyte density for the discharged negative half cell electrolyte results in lower frequencies. The frequency shift from cycle to cycle, which can be observed predominantly for the charged NHC, might indicate crossover processes. Since the method is temperature dependent, temperature has been also monitored and plotted in Figure 10 (b) but the observed frequency changes are not caused by changes in the electrolyte temperature.

The feasibility of EQCM measurements to identify crossover of different electrolyte components (active vanadium species, sulfuric acid, water) will be investigated further.

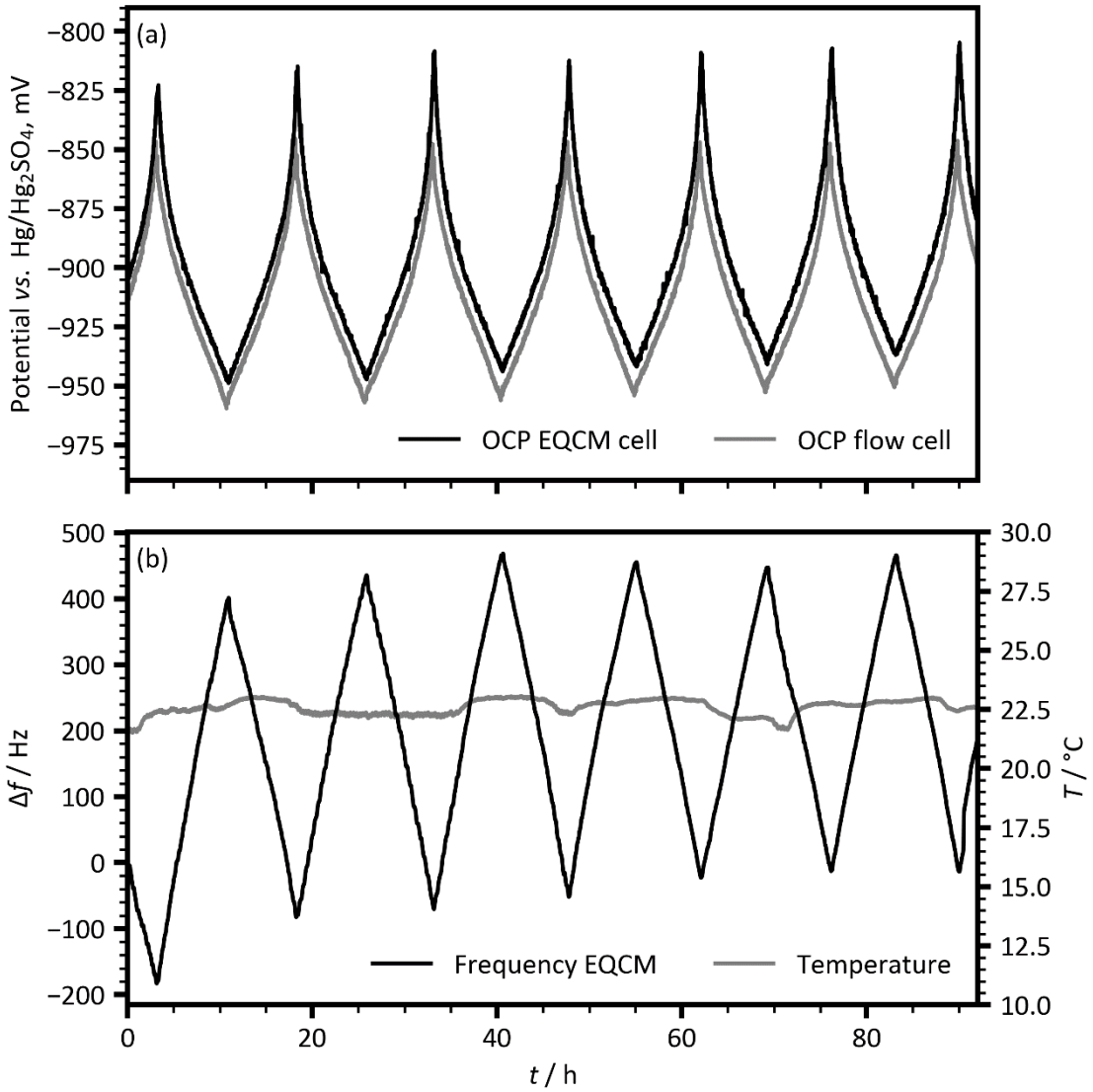

***Figure 10**. (a) Negative half cell: open circuit potential (OCP) measured in an EQCM cell compared to OCP measured in a flow cell at a glassy carbon rod. (b) Oscillation frequency of the quartz crystal changes in dependence on SOC, temperature of the negative half cell electrolyte is also shown*

Conclusions

Based on our first results for amperometric measurements in the electrolyte of a positive half cell of a vanadium flow battery laboratory test set up, we conclude this method is applicable for the *in situ* determination of the state of charge (SOC) of the positive half cell (PHC) electrolyte in vanadium flow batteries. A linear dependency of the current ratio (ratio of the measured oxidation and reduction currents, $\ln(I_{ox}/I_{red})$) on the concentration ratio (ratio of the concentration of the oxidised and reduced vanadium ions, $\ln(c_{ox}/c_{red})$) in the PHC has been found for several test setups and electrodes. A three-electrode setup using a carbon microelectrode as well as a glassy carbon (GC) rod and also a simplified two-electrode setup using two GC rods have been successfully applied for state of charge (SOC) monitoring in the PHC electrolyte. Additionally, SOC monitoring of negative half cell electrolytes using amperometric measurements will be investigated in the future. For all tested setups the choice of suitable oxidation and reduction potentials is essential for an accurate SOC determination. In addition to that, the ratio of diffusion coefficients and the long-term stability of the electrodes will also be considered in future research. Since all shown results have been gained *in situ* but with a stop and flow sampling of the electrolyte to ensure convection free amperometric

measurements, we will further investigate and develop a flow cell and a polarisation routine which allows an amperometric monitoring of the SOC in a flow-through mode. Since this method is simple concerning technical equipment and maintenance, we predict an applicability for field use in commercial vanadium flow batteries.

Summarizing the electrochemical quartz crystal microbalance (EQCM) results, we conclude that the redox potential respectively the open circuit potential of the negative half cell electrolyte can be monitored using a carbon coated quartz crystal. Furthermore, the oscillation frequency of this quartz crystal depends on the state of charge (SOC) of the electrolyte and therewith offers a new opportunity for SOC monitoring. As far as we know, an application of EQCM measurements for *in situ* SOC monitoring has not been published yet and we will further investigate the suitability of this technique for SOC determination as well as crossover identification and monitoring of different electrolyte components for the negative as well as the positive half cell of vanadium flow batteries. Also, the sensitivity to changes in temperature and concentration of the electrolyte will be investigated as well as the stability of the electrodes. Due to the complexity of the EQCM setup and its susceptibility for interferences we propose rather an application for laboratory research than for field use.

Acknowledgements: *We gratefully acknowledge funding by the German Federal Ministry for Economic Affairs and Climate Action. Furthermore, we kindly thank Christian Stolze (Friedrich Schiller University Jena) for scientific advice.*

References

[1] O. Nolte, I. A. Volodin, C. Stolze, M. D. Hager, U. S. Schubert, Trust is good, control is better: a review on monitoring and characterization techniques for flow battery electrolytes, *Materials Horizons* **8** (2021) 1866–1925. https://doi.org/10.1039/D0MH01632B

[2] I. Kroner, M. Becker, T. Turek, Monitoring the State of Charge of the Positive Electrolyte in a Vanadium Redox-Flow Battery with a Novel Amperometric Sensor, *Batteries* **5** (2019) 5. https://doi.org/10.3390/batteries5010005

[3] C. Stolze, P. Rohland, K. Zub, O. Nolte, M. D. Hager, U. S. Schubert, A low-cost amperometric sensor for the combined state-of-charge, capacity, and state-of-health monitoring of redox flow battery electrolytes, *Energy Conversion and Management X* **14** (2022) 100188. https://doi.org/10.1016/j.ecmx.2022.100188

[4] T. Haisch, H. Ji, C. Weidlich, Monitoring the state of charge of all-vanadium redox flow batteries to identify crossover of electrolyte, *Electrochimica Acta* **336** (2020) 135573. https://doi.org/10.1016/j.electacta.2019.135573

[5] T. Haisch, H. Ji, L. Holtz, T. Struckmann, C. Weidlich, Half cell State of Charge Monitoring for Determination of Crossover in VRFB—Considerations and Results Concerning Crossover Direction and Amount, *Membranes* **11** (2021) 232. https://doi.org/10.3390/membranes11040232

[6] L. Wei, T. S. Zhao, Q. Xu, X. L. Zhou, Z. H. Zhang, In-situ investigation of hydrogen evolution behavior in vanadium redox flow batteries, *Applied Energy* **190** (2017) 1112–1118. https://doi.org/10.1016/j.apenergy.2017.01.039

[7] H. Al-Fetlawi, A. A. Shah, F. C. Walsh, Modelling the effects of oxygen evolution in the all-vanadium redox flow battery, *Electrochimica Acta* **55** (2010) 3192–3205. https://doi.org/10.1016/j.electacta.2009.12.085

[8] Q. Luo, L. Li, W. Wang, Z. Nie, X. Wei, B. Li, B. Chen, Z. Yang, V. Sprenkle, Capacity Decay and Remediation of Nafion-based All-Vanadium Redox Flow Batteries, *ChemSusChem* **6** (2013) 268–274. https://doi.org/10.1002/cssc.201200730

[9] M. Skyllas-Kazacos, M. Kazacos, State of charge monitoring methods for vanadium redox flow battery control, *Journal of Power Sources* **196** (2011) 8822–8827. https://doi.org/10.1016/j.jpowsour.2011.06.080
[10] S. Ressel, F. Bill, L. Holtz, N. Janshen, A. Chica, T. Flower, C. Weidlich, T. Struckmann, State of charge monitoring of vanadium redox flow batteries using half cell potentials and electrolyte density, *Journal of Power Sources* **378** (2018) 776–783. https://doi.org/10.1016/j.jpowsour.2018.01.006
[11] T. Struckmann, P. Kuhn, S. Ressel, A combined in situ monitoring approach for half cell state of charge and state of health of vanadium redox flow batteries, *Electrochimica Acta* **362** (2020) 137174. https://doi.org/10.1016/j.electacta.2020.137174
[12] J. Geiser, H. Natter, R. Hempelmann, B. Morgenstern, K. Hegetschweiler, Photometrical Determination of the State-of-Charge in Vanadium Redox Flow Batteries Part I: In Combination with Potentiometric Titration, *Zeitschrift für Physikalische Chemie* **233** (2019) 1683–1694. https://doi.org/10.1515/zpch-2019-1379
[13] J. Geiser, H. Natter, R. Hempelmann, B. Morgenstern, K. Hegetschweiler, Photometrical Determination of the State-of-Charge in Vanadium Redox Flow Batteries Part II: In Combination with Open-Circuit-Voltage, *Zeitschrift für Physikalische Chemie* **233** (2019) 1695–1711. https://doi.org/10.1515/zpch-2019-1380
[14] N. Quill, C. Petchsingh, R. P. Lynch, X. Gao, D. Oboroceanu, D. Ní Eidhin, M. O'Mahony, C. Lenihan, D. N. Buckley, Factors Affecting Spectroscopic State-of-Charge Measurements of Positive and Negative Electrolytes in Vanadium Redox Flow Batteries, *ECS Transactions* **64** (2015) 23–39. https://doi.org/10.1149/06418.0023ecst
[15] D. N. Buckley, X. Gao, R. P. Lynch, N. Quill, M. J. Leahy, Towards Optical Monitoring of Vanadium Redox Flow Batteries (VRFBs): An Investigation of the Underlying Spectroscopy, *Journal of The Electrochemical Society* **161** (2014) A524–A534. https://doi.org/10.1149/2.023404jes
[16] X. Li, J. Xiong, A. Tang, Y. Qin, J. Liu, C. Yan, Investigation of the use of electrolyte viscosity for online state-of-charge monitoring design in vanadium redox flow battery, *Applied Energy* **211** (2018) 1050–1059. https://doi.org/10.1016/j.apenergy.2017.12.009
[17] M. Schilling, M. Braig, K. Köble, R. Zeis, Investigating the V(IV)/V(V) electrode reaction in a vanadium redox flow battery – A distribution of relaxation times analysis, *Electrochimica Acta* **430** (2022) 141058. https://doi.org/10.1016/j.electacta.2022.141058
[18] C. Stolze, J. P. Meurer, M. D. Hager, U. S. Schubert, An Amperometric, Temperature-Independent, and Calibration-Free Method for the Real-Time State-of-Charge Monitoring of Redox Flow Battery Electrolytes, *Chemistry of Materials* **31** (2019) 5363–5369. https://doi.org/10.1021/acs.chemmater.9b02376
[19] C. Stolze, M. D. Hager, U. S. Schubert, State-of-charge monitoring for redox flow batteries: A symmetric open-circuit cell approach, *Journal of Power Sources* **423** (2019) 60–67. https://doi.org/10.1016/j.jpowsour.2019.03.002
[20] B. J. Neyhouse, K. M. Tenny, Y.-M. Chiang, F. R. Brushett, Microelectrode-Based Sensor for Measuring *Operando* Active Species Concentrations in Redox Flow Cells, *ACS Applied Energy Materials* **4** (2021) 13830–13840. https://doi.org/10.1021/acsaem.1c02580
[21] P. M. Spaziante, M. Dichand, Estimation of the state of charge of a positive electrolyte solution of a working redox flow battery cell without using any reference electrode, Patent No. WO2014184617, 2013.
[22] G. Sauerbrey, Verwendung von Schwingquarzen zur Wägung dünner Schichten und zur Mikrowägung, *Zeitschrift für Physik* **155** (1959) 206–222. https://doi.org/10.1007/BF01337937 (in German)

[23] F. Tan, D.-Y. Qiu, L.-P. Guo, P. Ye, H. Zeng, J. Jiang, Y. Tang, Y.-C. Zhang, Separate density and viscosity measurements of unknown liquid using quartz crystal microbalance, *AIP Advances* **6** (2016) 095313. https://doi.org/10.1063/1.4963298

[24] S. Yenuganti, C. Zhang, H. Zhang, Quartz Crystal Microbalance for viscosity measurement with temperature self-compensation, *Mechatronics* **59** (2019) 189–198. https://doi.org/10.1016/j.mechatronics.2019.04.005

[25] Y. Ji, Z.-W. Yin, Z. Yang, Y.-P. Deng, H. Chen, C. Lin, L. Yang, K. Yang, M. Zhang, Q. Xiao, J.-T. Li, Z. Chen, S.-G. Sun, F. Pan, From bulk to interface: electrochemical phenomena and mechanism studies in batteries *via* electrochemical quartz crystal microbalance, *Chemical Society Reviews* **50** (2021) 10743–10763. https://doi.org/10.1039/D1CS00629K

[26] A. M. Cao-Paz, L. Rodríguez-Pardo, J. Fariña, J. Marcos-Acevedo, Resolution in QCM Sensors for the Viscosity and Density of Liquids: Application to Lead Acid Batteries, *Sensors* **12** (2012) 10604–10620. https://doi.org/10.3390/s120810604